



Report No. 487

**SUNLIGHT-MEDIATED REMOVAL OF EMERGING CONTAMINANTS IN
TREATMENT WETLANDS AND SURFACE WATERS**

By
Tarek N. Aziz
Arpit Sardana

Department of Civil, Construction, and Environmental Engineering
North Carolina State University
Raleigh, North Carolina

September 4, 2020

UNC-WRRI-487

The research on which this report is based was supported by funds provided by the Urban Water Consortium through the North Carolina Water Resources Research Institute.

The views and conclusions contained in this document are those of the authors and should not be interpreted as necessarily representing the official policies, either expressed or implied, of the U.S. Government, the North Carolina Water Resources Research Institute or the State of North Carolina.

This report fulfills the requirements for a project completion report of the North Carolina Water Resources Research Institute. The authors are solely responsible for the content and completeness of the report.

WRRI Project No. 19-05-U
September 4, 2020

Project Report to the Water Resources Research Institute
of
The University of North Carolina System
For Research Entitled

Sunlight-Mediated Removal of Emerging Contaminants in Treatment Wetlands and Surface Waters

WRI Project: 19-05-U
March 1, 2019 - June 30, 2020

Faculty Sponsor:
Tarek N. Aziz, PhD
Assistant Professor, Department of Civil, Construction, and Environmental Engineering
North Carolina State University
tnaziz@ncsu.edu

Student Investigator:
Arpit Sardana, PhD Candidate
Graduate Research Assistant, Department of Civil, Construction, and Environmental Engineering
North Carolina State University
asardan@ncsu.edu

Date Submitted: September 4, 2020
PINS Number: 94217

Keywords: treatment wetlands, emerging contaminants, photochemistry

ABSTRACT

In this project, we evaluated the photodegradation kinetics of wastewater derived emerging contaminants in treatment wetlands. We used dissolved organic matter (DOM) characterization tools and simulated irradiation experiments to investigate the relationship between photochemical behavior and wetland processing of wastewater effluents. Samples were collected from a treatment wetland site and a wastewater treatment plant (WWTP) in North Carolina. Cimetidine (CME), amoxicillin (AMX), 17 α -ethinyl-estradiol (EE2), and atenolol (ATL) were selected as target contaminants to evaluate photoreactivity of sampled waters. Target compounds were individually dissolved in the collected samples and their decay during irradiation was measured using HPLC methods. The direct photolysis photodegradation rates and quantum yields were calculated for AMX, EE2, and ATL, as these pharmaceuticals have been shown to undergo both direct and indirect photodegradation in sunlit waters. Photochemically produced reactive intermediates, such as excited triplet states of dissolved organic matter ($^3\text{DOM}^*$), singlet oxygen ($^1\text{O}_2$), and hydroxyl radical ($\cdot\text{OH}$) were found to be substantially sensitized by both treatment wetland samples and WWTP effluents. $\cdot\text{OH}$ acted as the main photoreactant responsible for the phototransformation of AMX, ATL, and EE2. Photodegradation of CME was entirely due to singlet oxygen formation from irradiated DOM. Phototransformation rates and quantum yield coefficients were calculated to estimate the photochemical fate of the pharmaceuticals in sampled waters. Overall, photodegradation was fastest for CME, followed by EE2, and then AMX and ATL. It was observed that photoreactivity was higher in lagoon treated wastewaters than compared to vegetated wetland cells and secondary wastewater effluents. Some samples were observed to have an enhanced $\cdot\text{OH}$ formation yield which led to significantly higher phototransformation rates. This was suggested to be due to the activity of photo-Fenton reactions and DOM dependent hydroxylators. Optical indices for DOM characteristics were computed from ultraviolet–visible (UV-Vis) spectroscopy and excitation-emission matrix (EEM) fluorescence spectroscopy. ATL and EE2 photoreactivity was observed to be negatively correlated to humic and fulvic DOM components. The absorbance ratio (E2:E3) was found to be positively correlated only to CME phototransformation rates. Results from this study suggest that plant-derived organic matter from vegetated wetland cells can decrease photoreactivity of treatment wetland waters.

Table of Contents

1. Introduction	1
2. Methods	3
2.1 Sampling.....	3
2.2 Irradiation experiments	5
2.3 Analyses	6
2.4 Photochemical modelling.....	7
3. Results and discussion	8
3.1 Water quality and dissolved organic matter composition	8
3.2 Phototransformation rates of pharmaceuticals	10
3.3 Optical properties and photoreactivity relationships.....	13
3.4 Coupling photochemical processes and wetland design	16
4. Conclusions	17
References.....	19

1. Introduction

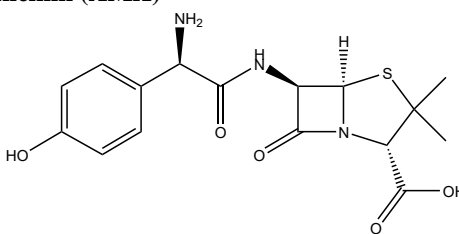
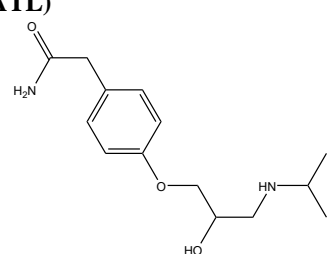
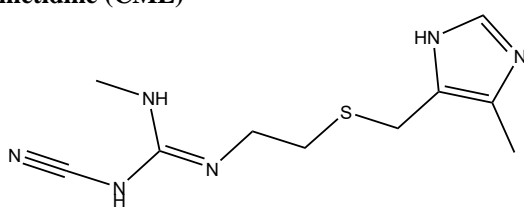
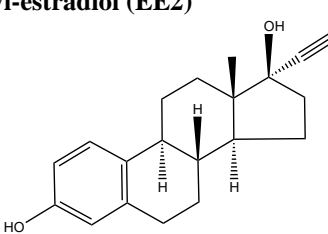
Multiple nationwide USGS surveys have detected the presence of wastewater-derived trace organics such as pharmaceuticals and personal care products in our surface waters (Focazio et al., 2008; Glassmeyer et al., 2017; Kolpin et al., 2002). These contaminants of emerging concern (CECs) are known to impair aquatic health (Brodin et al., 2013; Schwarzenbach et al., 2006). Presence of these CECs at ng/L to µg/L concentration levels can lead to altered fish behavior, population loss, reproductive disruption, and other unknown ecotoxicological effects (Brodin et al., 2013; FENT et al., 2006; Kidd et al., 2007; Schwarzenbach et al., 2006; Snyder et al., 2003; Vajda et al., 2008). Conventional wastewater treatment cannot treat many CECs due to their recalcitrance to biological processes (Snyder et al., 2003). Surface flow constructed wetlands (CWs) are suitable treatment alternatives which can be used for polishing wastewater effluents or as complete treatment systems in smaller communities (Jasper et al., 2013; Matamoros and Salvadó, 2012; Sardana et al., 2019; Silverman et al., 2015). Biological and abiotic processes in these systems influence the fate and transport of CECs (Verlicchi and Zambello, 2014; Zhang et al., 2018). Photodegradation has specifically been shown to significantly contribute to CECs removal in full scale surface flow wetlands (Andreozzi et al., 2003; Matamoros et al., 2008). While technologies such as advanced oxidation processes, activated carbon, and reverse osmosis can remove CECs from wastewater, these processes are resource intensive and challenging for conventional wastewater treatment facilities (Jasper and Sedlak, 2013; Pereira et al., 2007; Rosario-Ortiz et al., 2010; Snyder et al., 2003). Photochemical processes can be harnessed in treatment wetland systems to develop a sustainable, low-cost approach for CECs removal.

The kinetics of photodegradation is dependent on the dissolved organic matter (DOM) composition, irradiation intensity, and photochemical properties of the CEC (Challis et al., 2014; Karpuzcu et al., 2016). Direct photodegradation rates are dependent on the intensity of light absorbed by the exposed water column and the reaction quantum yield (Schwarzenbach et al., 2002). In addition to direct photodegradation, photoproducted reactive intermediates (PPRIs) are produced during the interaction of sunlight with various dissolved constituents in the water. This leads to a significant rate of indirect photodegradation and can play a dominant role in CECs degradation. The DOM quantity and quality of the water matrix plays a crucial role in the photogeneration efficiency of PPRIs such as triplet excited states of CDOM (${}^3\text{CDOM}^*$), singlet oxygen (${}^1\text{O}_2$), hydroxyl radical (${}^{\bullet}\text{OH}$), and carbonate radical ($\text{CO}_3^{\bullet-}$). DOM can either act as a photosensitizer to generate PPRIs or can inhibit indirect photodegradation of CECs by quenching PPRIs precursors and acting as an antioxidant (Chu et al., 2015; Sharpless et al., 2014a; Wenk et al., 2011). The ability of dissolved organic materials in treatment wetlands to photodegrade CECs has not been clearly understood and is the central objective of this work. Natural processes occurring in wetland cells modify the composition of effluent organic matter (EfOM) (Barber et al., 2001; Lee et al., 2014). Biological functioning, plant senescence, and photobleaching, all process EfOM to a more terrestrial humic-like form (Barber et al., 2001; Pinney et al., 2000). This transition to an allochthonous natural organic matter (NOM) composition can limit the photogeneration of PPRIs due to light screening, lower photogeneration yields, intermediate quenching,

and antioxidation effects (Coelho et al., 2011; McCabe and Arnold, 2018; Miller and Chin, 2002; Peterson et al., 2012; Wenk et al., 2019).

This study aims to clarify, and compile photodegradation performance of whole water samples collected from wastewater treatment lagoons, open-water ponds, vegetated wetland cells, and wastewater treatment facilities. The DOM processing of wastewater effluents in treatment wetlands is understood to play a key role in photochemical behavior and reaction kinetics. We hypothesize that photosensitization reactions in treatment wetland cells are influenced by the presence of plant derived organic matter and effluent processing by wetland features. Leaching of humic substances from vegetated cells and transition of wastewater to a more terrestrial-like DOM profile has been suggested to inhibit reactive intermediates photogeneration (Wenk et al., 2019). A net gain or loss of photodegradation potential due to varying DOM properties is evaluated in this photochemical investigation. Understanding the extent by which DOM characteristics influence phototransformation rates will support the design of open-water cell unit processes. Irradiation experiments with pharmaceuticals as test compounds – amoxicillin (AMX), atenolol (ATL), cimetidine (CME), and 17 α -ethinyl-estradiol (EE2) are used to evaluate the influence of wetland processes on phototransformation rates (Table 1). Optical properties and water chemistry measurements are used to characterize the processing of wastewater through different wetland cells. The four pharmaceuticals selected in this study are known to react with different tendencies with $^1\text{O}_2$, $^{\bullet}\text{OH}$, and $^3\text{CDOM}^*$. Photosensitization pathways for the pharmaceuticals are described in connection with photosensitizer characteristics and sampling location. Predictive relationships and correlations between optical properties and photodegradation rates are developed to understand the DOM mediated photosensitization in treatment wetland systems.

Table 1: Structure and properties of the target pharmaceuticals.

structure	solubility in water	pK _a	log K _{ow}	references
<p>amoxicillin (AMX)</p> 	400 mg L ⁻¹	2.7, 9.6	7.5, 0.87	(Yoon et al., 2004), (Cass et al., 2003)
<p>atenolol (ATL)</p> 	soluble	9.6	0.16	(Liu and Williams, 2007), (Küster et al., 2007)
<p>cimetidine (CME)</p> 	freely soluble	7.1	0.57	(Latch et al., 2003), (Zenobio et al., 2015)
<p>17α-ethinyl-estradiol (EE2)</p> 	4.8 mg L ⁻¹	10.5	3.67	(Ren et al., 2016)

2. Methods

2.1 Sampling

Wetland waters were collected in September 2018 from lagoons, open-water ponds, and vegetated cells of a treatment wetland site operated by the Town of Walnut Cove, North Carolina. The eleven sampling locations at the site included distribution outlets, surface waters, and a river location downstream of utility discharge (Figure 1). The site has been operational since 1996 and treats approximately 0.3 MGD of municipal wastewater. Sewage is pumped to a series of lagoons and shallow open-water cells, followed by release into cattail (*Typha latifolia*) vegetated wetland cells.

Additional site characteristics and the functioning of treatment wetland processes have been described previously (Sardana et al., 2019).

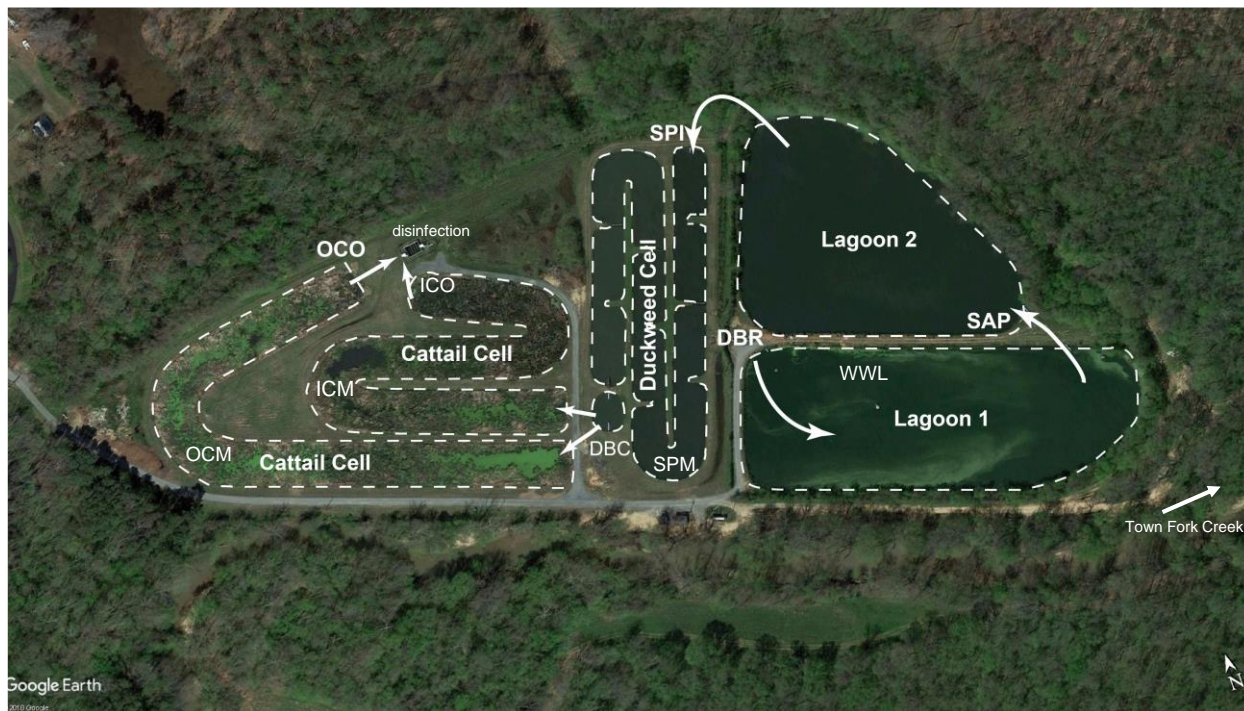


Figure 1: Treatment wetland site at Walnut Cove, NC.

Labels for sampling locations - DBR (Distribution Box Raw Sewage), WWL (Wastewater Lagoon), SAP (Second Aeration Pond), SPI (Serpentine Pond Inlet), SPM (Serpentine Ponds Midpoint), DBC (Distribution Box Cattail cells), ICM (Inner Cattails Midpoint), ICO (Inner Cattail Cell Outlet), OCM (Outer Cattail Cell Outlet Midpoint), OCO (Outer Cattail Cell Outlet), and TFD (Town Fork Creek Downstream).

In November 2019, effluent samples were collected from five different locations across the wastewater treatment train of the Neuse River Resource Recovery Facility (NRRRF) in Raleigh, NC (Figure 2). The 75 MGD facility has an equalization basin and uses conventional primary treatment units for screening municipal sewage. The biological nutrient removal basins have activated sludge processes and anoxic zones for efficient nitrogen removal. Secondary effluents are treated through denitrification filters and UV disinfection before discharge. Grab samples from the two utilities were collected in certified amber containers and stored on ice during transportation. Glass-fiber filters with a 0.7 μm pore size were combusted at 550 $^{\circ}\text{C}$ and used to pre-filter samples. Samples were then filter-sterilized through 0.2 μm pore size membrane filters (Durapore[®], MilliporeSigma) and stored in the dark at 4 $^{\circ}\text{C}$ in amber glass bottles. Blended samples were additionally prepared by mixing filtered samples (v/v ratio of 50:50) to evaluate effect of combining diverse DOM compositions. Irradiation experiments, DOM characterizations, and water chemistry measurements were performed on the collected whole water matrices.

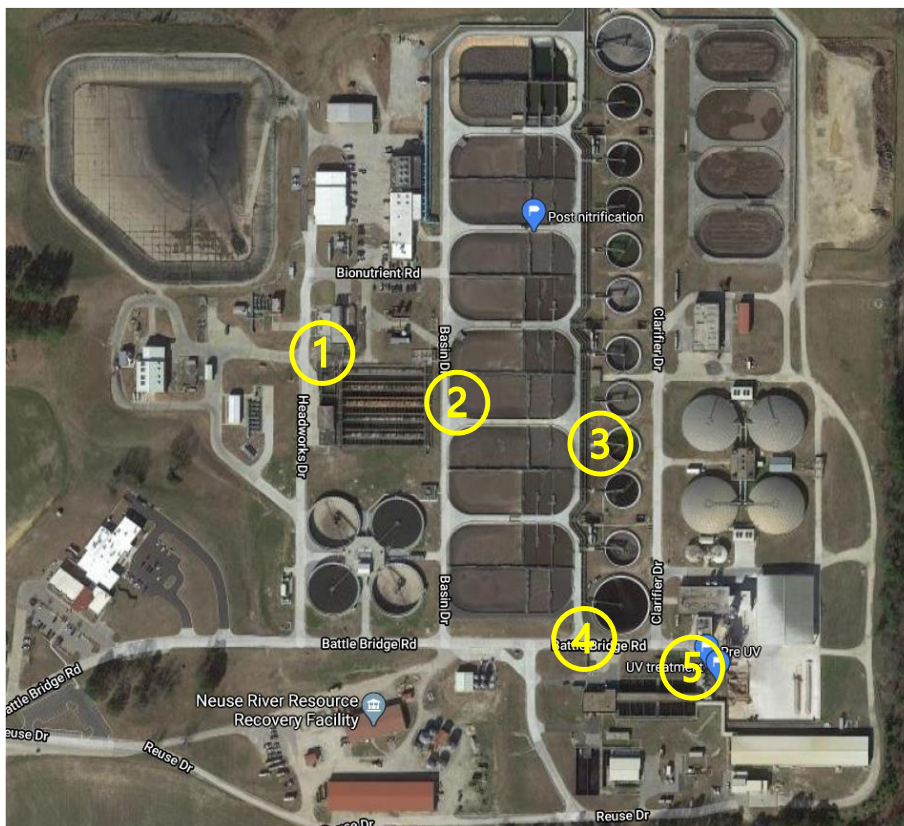


Figure 2: Neuse River Resource Recovery Facility (NRRRF), Raleigh, NC. Locations 1 and 2 are primary effluents, the rest are secondary effluents.

2.2 Irradiation experiments

An ATLAS SUNTEST CPS+ solar simulator with a natural sunlight filter (< 290 nm) and an air ventilation system was used for the irradiation of water samples spiked with target compounds. The sunlight simulator has a 1500 W xenon lamp and an irradiance range of 30-65 W/m² at 300-400 nm range or 250-765 W/m² at 300-800 nm range. For all irradiation experiments the total irradiance for the 300-400 nm range was set at 30 W/m². For the 300-400 nm wavelength range, a one-sun irradiance equivalent is 60 W/m² for terrestrial solar radiation (International Commission on Illumination, CIE 085-1989). Samples were irradiated in quartz test tubes (13 x 100 mm, Ace Glass) with an effective optical path length of 1.12 cm (Leifer, 1989). The tubes were sealed during irradiation by rubber septa and held within the irradiation chamber at a 30° angle from horizontal (McCabe and Arnold, 2018). The chamber temperature during irradiance experiments was maintained below 30 °C by circulating ambient air. The design of irradiation experiments represents near surface conditions of sunlit waters. An actinometer solution of 10 μM *p*-nitroanisole (PNA) and 5 mM pyridine (pyr) was used to calculate the spectral photon irradiance (I_{λ} , mol-photons L⁻¹ s⁻¹ nm⁻¹) and total photon irradiance ($I_{\lambda, tot}$ mol-photons L⁻¹ s⁻¹) of the lamp incident on the samples. Irradiance calculations were performed over the range of 275-800 nm using the relative spectral irradiance provided by ATLAS and the procedure outlined in Sharpless et al., (2014). The PNA-pyr quantum yield relationship updated by Laszakovits et al., (2017) was used to calculate total photon irradiance, which was estimated to be 1.45E-4 mol-photons L⁻¹ s⁻¹.

Four target pharmaceutical compounds were selected for irradiation experiments – atenolol (ATL), amoxicillin (AMX), cimetidine (CME), and 17 α -ethinyl-estradiol (EE2). These were selected as test compounds as these are wastewater derived organic micropollutants which phototransform via photosensitization reactions with $\cdot\text{OH}$, $^3\text{DOM}^*$, $^1\text{O}_2$, and $\cdot\text{CO}_3^-$ (Challis et al., 2014; Jasper and Sedlak, 2013; Song et al., 2008). The four pharmaceuticals were individually spiked in the collected water samples and irradiated in at least duplicate test tubes to estimate phototransformation rates ($k_{obs-photo}$, time^{-1}) under simulated sunlight. Irradiation solutions were prepared in volumetric flasks by dissolving a nominal volume of stock pharmaceutical solution into water samples to give a known initial concentration (C_0) at mg/L level. The photo-decay of the pharmaceuticals was tracked by sampling aliquots (200 μL) from the test tubes at regular intervals and measuring concentration (C_t) using a high performance liquid chromatography (HPLC) system. Irradiation experiments lasted between 1 – 10 hrs and the decay was modeled as a pseudo first-order reaction (Equation 1) with an exponential transformation rate ($k_{obs-photo}$, time^{-1}).

$$C_t = C_0 e^{-(k_{obs-photo})t}$$

Equation 1

HPLC methods for each pharmaceutical were adopted from published studies which used isocratic elution with a C-18 reversed phase column and UV absorbance detection (Latch et al., 2003; Ren et al., 2016; Wang et al., 2012; Xu et al., 2011). The direct photolysis of pharmaceuticals was also analyzed by performing similar experiments with high purity water ($> 18 \text{ M}\Omega$). The pH of all samples was near neutral and no water chemistry adjustments were made during the preparation of irradiation solutions. Dark controls were prepared by covering the test tubes with foil and measuring concentration over the experiment duration. Only amoxicillin demonstrated decay in the dark controls, and this was attributed to DOM sorption and hydrolysis (Xu et al., 2011). Additional solutions were prepared for irradiation experiments by dissolving 1% (v/v) isopropyl alcohol (IPA) or 10 mg/L NO_3^- in the sampled waters. IPA quenches $\cdot\text{OH}$ formed during irradiation, whereas, NO_3^- sensitizes the photogeneration of $\cdot\text{OH}$.

2.3 Analyses

The concentration of pharmaceuticals in aliquots from photochemical experiments was determined by a Shimadzu Prominence HPLC system. Isocratic elution methods were developed, and chromatograms were detected using a UV-Vis diode array detector. Details about mobile phase, column, and detection wavelengths were based on previous studies which have used similar HPLC methods to determine photochemical analytes at mg/L concentrations from simulated irradiation experiments (Bodhipaksha et al., 2017; Ren et al., 2019b; Wang et al., 2012; Xu et al., 2011). Ultraviolet–visible (UV-Vis) absorbance and Excitation Emission Matrix (EEM) fluorescence of water samples were performed on a HORIBA Aqualog. Primary effluents from the wastewater utility ($\text{DOC} > 25 \text{ mg-C L}^{-1}$) were diluted with high purity water prior to spectral measurements. All samples had absorbance lower than 0.6 cm^{-1} at 254 nm, such that inner filter effects during measurements were limited (McCabe and Arnold, 2018). The range of excitation wavelength for EEM scan was 240 to 650 nm at an increment of 3 nm and the emission range was 245.7 to 828.05

nm at an emission increment of 2.2 nm. Spectral scans were processed using the Aqualog software to correct inner filter effect, remove Rayleigh scattering, and normalize instrument intensity to standardized water Raman units (RU). The staRdom R package was used to extract and tabulate all optical parameters (Pucher et al., 2019). Fluorescence indices, absorption coefficients (a_λ), and UV-Vis spectral parameters (E2:E3 ratio, spectral slope ratio S_R , and specific UV absorbance at 254 nm $SUVA_{254}$) were calculated using peak picking and regression procedures (Helms et al., 2013; Weishaar et al., 2003). Biological index (BIX), humification index (HIX), and fluorescence index (FI) are dimensionless fluorescence parameters which were also computed to differentiate and compare sources and nature of DOM composition (Huguet et al., 2009; McKnight et al., 2001; Ohno*, 2002). Peak intensities from five different fluorescing areas of the EEM were obtained - B (tyrosine-like, protein-like), T (tryptophan-like, protein-like), A (UV humic-like), M (marine humic-like), and C (visible humic-like / fulvic-like) (Coble, 1996). Ionic species of nitrate, ammonia, and iron were measured using established colorimetric techniques for wastewater effluents. The ferrozine method was used to measure iron concentration (HACH method 8147). A Shimadzu TOC analyzer was used to measure dissolved organic carbon (DOC) concentration of filtered samples. Field measurement of pH, dissolved oxygen (DO), and conductivity were performed on site with unfiltered samples using a hand-held probe (Thermo Scientific Orion Star A). Statistical analysis of possible correlations between phototransformation rates, water chemistry parameters, and DOM optical properties was performed in R by computing the Spearman' rank correlation matrix (Harrell Miscellaneous Hmisc R package).

2.4 Photochemical modelling

The total rate of light absorption by sample DOM was calculated using the lamp spectral irradiance, I_λ , from PNA-pyr actinometry (Equation 2). a_λ (m^{-1}) is the decadic absorbance of irradiated samples and z is the effective path length (m) of the quartz test tubes used during experiments.

$$R_a = \sum_{\lambda=275 \text{ nm}}^{650 \text{ nm}} I_\lambda (1 - 10^{-a_\lambda \cdot z})$$

Equation 2

Direct photolysis quantum yields (Φ_{direct}) for amoxicillin, atenolol, and 17 α -ethinyl-estradiol were calculated using wavelength dependent molar extinction coefficients and by proportioning actinometer photolysis with pharmaceutical photodegradation in pure waters (Andreozzi et al., 2003). For the purpose of normalizing photoreactivity potential of samples with diverse absorption spectra, quantum yield coefficients $f_{pharmaceutical}$, ($mol\text{-photons}^{-1} L$) (Equation 3) for each target pharmaceutical were estimated (Bodhipaksha et al., 2017).

$$f_{pharmaceutical} = \frac{k_{obs} - k_{direct,photo} - k_{DOM \text{ sorption}}}{R_a}$$

Equation 3

Photodegradation rates (day^{-1}) of pharmaceuticals in an open-water wetland cell as a function of depth and season were also estimated. Day-averaged solar irradiance values for June 21st and December 22nd for 40°N latitude were used as reference for seasonal variation (Apell and McNeill, 2019). Light attenuation below the water surface was calculated for an absorption spectra representative of wetland waters.

3. Results and discussion

3.1 Water quality and dissolved organic matter composition

A total of sixteen samples from the Walnut Cove wetland site and the NRRRF wastewater utility were analyzed for water chemistry measurements and DOM optical properties (Table 2 and Table 3). DOC levels and absorption coefficient, a_{254} , decreased as wastewater passed through wetland cells and treatment basins. Optical proxies to DOM molecular weight, E2:E3 and S_R , did not vary significantly between locations at the two sites. SUVA₂₅₄, which is an indicator of DOM aromaticity, was higher in the wetland site compare to the wastewater facility. Ammonia (NH_4^+) concentrations of samples from wetland processes averaged about 10 mg/L. The ammonification of organic nitrogen can also be a source of ammonia release in surface flow vegetated wetland cells (Vymazal, 2007). Except for a partially denitrified secondary effluent at NRRRF, nitrate (NO_3^-) was < 1 mg/L throughout the treatment utilities, implying that nitrate mediated photosensitization of $\cdot\text{OH}$ is limited for these samples. The average concentration of dissolved iron (Fe) in filtered samples from Walnut Cove was 0.52 mg/L as compared to 0.19 mg/L of NRRRF. The presence of iron during irradiation of DOM solutions can lead to additional formation of $\cdot\text{OH}$ through photo-Fenton reactions between photogenerated hydrogen peroxide (H_2O_2) and Fe(II) (Vermilyea and Voelker, 2009).

Table 2: Average and standard deviation of water quality and UV-Vis absorbance parameters at different locations.

variable (units)	Walnut Cove wetland site				NRRRF	
	sewage (n = 1)	lagoon treated wastewater (n = 5)	vegetated wetland cells (n = 4)	downstream discharge (n = 1)	WWTP primary effluent (n = 2)	WWTP secondary effluent (n = 3)
DOC (mg-C L ⁻¹)	6.28	9.84 ± 0.74	8.96 ± 1.00	4.06	25.60 ± 0.30	7.14 ± 0.21
Fe (mg L ⁻¹)	0.18	0.64 ± 0.44	0.46 ± 0.32	0.49	0.33 ± 0.22	0.09 ± 0.05
a₂₅₄ (Napierian m ⁻¹)	45.15	75.18 ± 28.83	68.98 ± 11.40	36.90	80.52 ± 6.62	41.43 ± 0.66
E2:E3	3.39	4.47 ± 0.48	4.67 ± 0.39	4.71	3.96 ± 0.03	4.46 ± 0.00
S_r	0.94	1.00 ± 0.13	0.98 ± 0.17	0.74	1.20 ± 0.11	0.84 ± 0.04
SUVA₂₅₄ (decadic L mg- C ⁻¹ m ⁻¹)	3.12	3.31 ± 0.98	3.34 ± 0.26	3.94	1.37 ± 0.10	2.52 ± 0.04
NO₃⁻ (mg L ⁻¹)	1.70	0.32 ± 0.22	0.33 ± 0.05	0.10	0.40 ± 0.14	1.37 ± 1.85
NH₄⁺ (mg L ⁻¹)	15.00	11.00 ± 3.81	10.50 ± 5.45	1.00	40.00 ± 1.41	0.00 ± 0.00
pH	7.34	7.22 ± 0.64	6.82 ± 0.08	7.17	-	-
DO (mg L ⁻¹)	0.28	5.27 ± 4.57	4.74 ± 1.28	7.65	-	-
conductivity (μS cm ⁻¹)	609.70	453.02 ± 17.73	406.53 ± 4.71	194.90	-	-

Rate of light absorption and fluorescence indices of the DOM samples collected from the utilities are summarized in Table 3. Spectral characteristics were used to track DOM processing through the treatment systems and to evaluate the influence of DOM composition on photodegradation reactions. Raw sewage and primary effluents absorbed more light than treated wastewater samples and had fluorescence metrics indicative of a predominantly microbially sourced organic matter. Untreated wastewater samples had the highest biological index (BIX) and fluorescence index values (FI) with the lowest humification index (HIX). Bacterial-soluble microbial products were the dominating fluorophores in wastewater and led to a relatively intense emission signature in the B (tyrosine-like, protein-like) and T (tryptophan-like, protein-like) regions of the EEM (Chen et al., 2003). As wastewater DOM processed through wetland cells the intensity for the A (UV humic-like), M (marine humic-like), and C (visible humic-like / fulvic-like) EEM regions gradually increased. The leaching of plant-derived organic matter from the vegetated cells increased the terrestrial-humic like DOM characteristics of wetland effluents (Maie et al., 2006; Pinney et al., 2000; Sardana et al., 2019).

Table 3: Average and standard deviation of rate of light absorption and EEMs fluorescence indices.

variable (units)	Walnut Cove wetland site				NRRRF	
	sewage (n = 1)	lagoon treated wastewater (n = 5)	vegetated wetland cells (n = 4)	downstream discharge (n = 1)	WWTP primary effluent (n = 2)	WWTP secondary effluent (n = 3)
R_a (mol- photons L ⁻¹ s ⁻¹)	7.00E-06	1.00E-05 ± 5.49E-06	6.96E-06 ± 2.33E-06	2.95E-06	1.22E-05 ± 1.74E-06	4.20E-06 ± 7.95E-08
BIX	0.92	0.87 ± 0.04	0.84 ± 0.02	0.75	0.91 ± 0.12	0.82 ± 0.05
B peak (R.U.)	1.75	1.64 ± 0.49	1.45 ± 0.66	0.34	2.69 ± 0.71	0.90 ± 0.02
T peak (R.U.)	2.21	1.77 ± 0.62	1.58 ± 0.75	0.34	3.68 ± 0.96	1.24 ± 0.02
A peak (R.U.)	1.55	2.38 ± 0.18	2.53 ± 0.13	1.23	2.80 ± 0.26	2.49 ± 0.10
M peak (R.U.)	1.26	1.69 ± 0.15	1.78 ± 0.11	0.81	2.38 ± 0.25	2.12 ± 0.10
C peak (R.U.)	1.48	1.51 ± 0.11	1.55 ± 0.07	0.69	2.29 ± 0.05	2.61 ± 0.32
FI	1.79	1.56 ± 0.05	1.49 ± 0.02	1.38	1.70 ± 0.03	1.81 ± 0.06
HIX	0.61	0.72 ± 0.05	0.75 ± 0.06	0.84	0.63 ± 0.04	0.80 ± 0.00

3.2 Phototransformation rates of pharmaceuticals

The direct photodegradation rate constants in pure waters were calculated for amoxicillin (AMX), atenolol (ATL), and 17 α -ethinyl-estradiol (EE2) to be 0.008 hr⁻¹, 0.004 hr⁻¹, and 0.035 hr⁻¹, respectively. Cimetidine does not degrade via direct photolysis and only undergoes indirect photodegradation via photogenerated ¹O₂ in sunlit waters (Bodhipaksha et al., 2017). The direct photolysis quantum yields (Φ_{direct} , mol mol-photons⁻¹) were estimated using the molar extinction coefficients of the pharmaceuticals and the spectral irradiance characteristics during irradiation experiments. The Φ_{direct} of AMX, ATL, and EE2 was 6.63E-04, 2.74E-03, and 1.56E-02, respectively. A similar Φ_{direct} value has been reported for EE2 by Ren et al., (2016) but AMX and ATL estimates in previous studies were higher than noted in this study. (Andreozzi et al., 2004; Yamamoto et al., 2009) This could be due to variation in absorption spectra, actinometry relationships, and experimental conditions. In environmental waters, indirect photodegradation is the major phototransformation pathway for the selected pharmaceuticals. The photodegradation rates observed in the wetland waters and wastewater effluents sampled for this study are illustrated in Figure 3. The phototransformation rates were normalized to the DOC of the respective samples in order to compare photoreactivity between samples grouped by site and location. Overall, EE2 photodegraded the fastest, followed by CME, AMX, and ATL. CME photodegradation observed in waters collected from the two sites show similar decay rates when normalized with respect to DOC. However, there is significant variation in the magnitude of the phototransformation rates for the remaining test compounds. Mean photodegradation rates for the other three pharmaceuticals are slightly higher in open water lagoons and ponds when compared to vegetated cells. Moreover,

some samples exhibit higher levels of decay than compared to similarly grouped samples. This could be due to dissimilar photosensitization efficiencies in different DOM matrices.

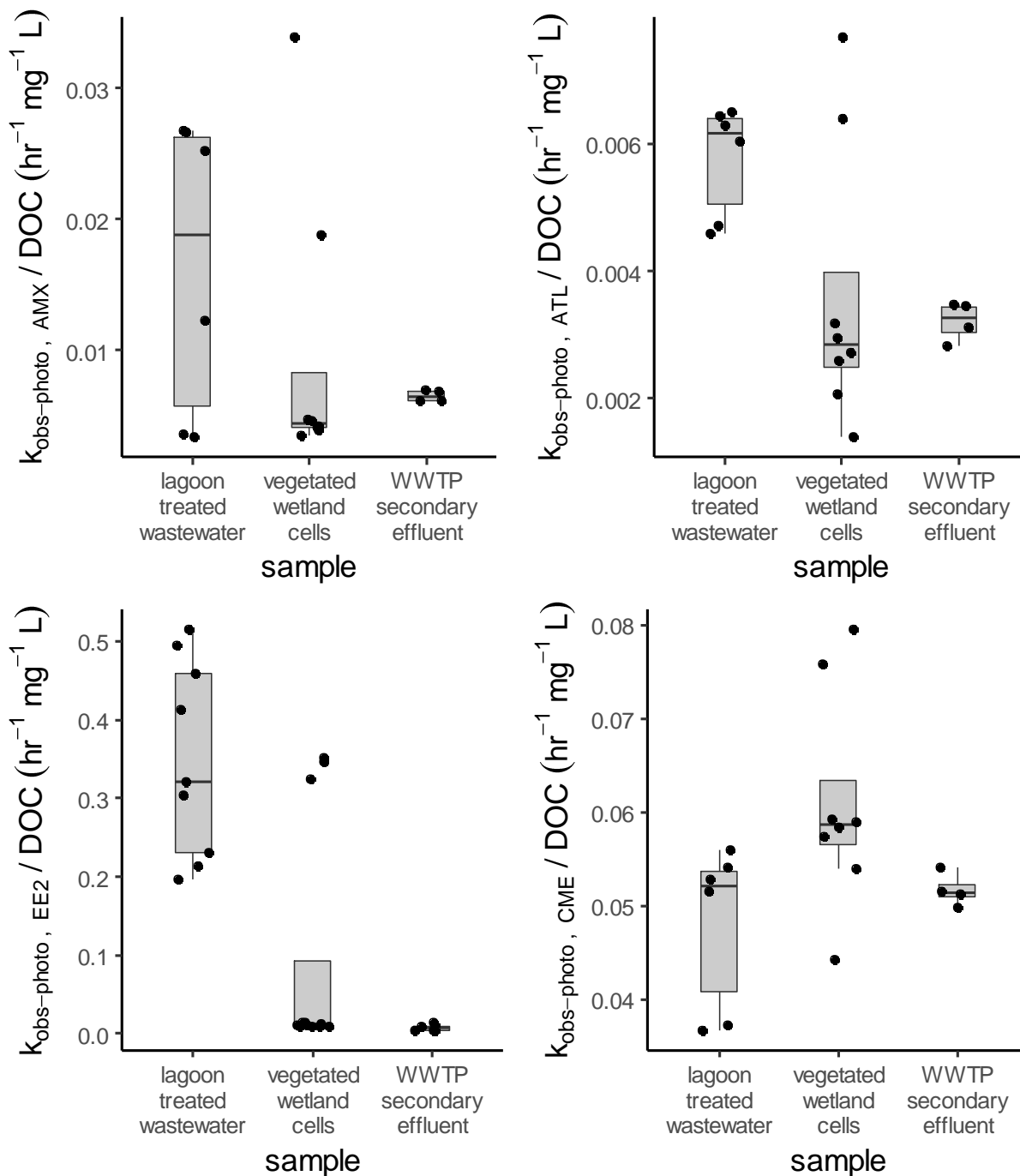


Figure 3: Carbon-normalized photodegradation rate constants for amoxicillin (AMX), atenolol (ATL), 17 α -ethynyl-estradiol (EE2), and cimetidine (CME) observed for sampled whole waters.

Previous studies focusing on wastewater effluents, pond waters, and natural organic matter isolates have reported the different photosensitization reactions responsible for pharmaceutical photo-

decay. In wastewater effluents, ATL is expected to degrade mainly by reacting with photogenerated $\cdot\text{OH}$ (Jasper and Sedlak, 2013). Whereas, the major photosensitization pathway for AMX was found to be a reaction with $^3\text{DOM}^*$ species in both natural organic matter isolates and wastewater effluents (Andreozi et al., 2004; Xu et al., 2011). For EE2, both reactive oxygenates species ($\cdot\text{OH}$, H_2O_2 , $^1\text{O}_2$) and $^3\text{DOM}^*$ contribute towards photodegradation (Ren et al., 2016). Fulvic acid solutions have been shown to photodegrade EE2 faster than humic acid solutions, with $\cdot\text{OH}$ being the primary contributor in humic acids and $^3\text{DOM}^*$ dictating more in fulvic acids (Ren et al., 2019a).

To further elucidate the contribution of different reactive intermediates in photodegrading pharmaceuticals, quencher experiments were performed with isopropyl alcohol (IPA) in selected wetland waters. 1% IPA was dissolved in DOM solutions prior to irradiation to scavenge photogenerated $\cdot\text{OH}$ and experiments were performed as previously described. In the absence of reactivity with $\cdot\text{OH}$, the photodegradation rates of AMX, ATL, and EE2 decreased, thereby distinguishing the contribution of $\cdot\text{OH}$ mediated photodegradation from total observed photodegradation (Figure 4). ATL phototransformation in water samples was almost entirely due to $\cdot\text{OH}$ reactivity as rates decreased to direct photolysis levels in the presence of IPA (Jasper and Sedlak, 2013; Zeng et al., 2012). Some whole water samples (DBC, ICO, SPM) had a significantly higher photosensitization ability, which got inhibited in solutions with 1% IPA. The enhanced $\cdot\text{OH}$ photoreactivity in these samples could be due to a high yield of $\cdot\text{OH}$ through photo-Fenton reactions and Fe(III)-DOM complexation reactions or due to the formation of H_2O_2 dependent hydroxylating photoreactants (Bodhipaksha et al., 2017; Page et al., 2011a; Zeng et al., 2012). The drastic difference in phototransformation rates between samples was most evident in the case of EE2 (~10x increase) and to a lesser degree in ATL (~3x increase), and AMX (~4x increase). The % removal of AMX by $\cdot\text{OH}$ was 6 – 94 % while % removal of EE2 by $\cdot\text{OH}$ was 46 – 91 %. $^3\text{DOM}^*$ plays an important role in the photodegradation of AMX in DOM matrices while EE2 photosensitization is collectively influenced by $^3\text{DOM}^*$, $\cdot\text{OH}$, $^1\text{O}_2$, and H_2O_2 pathways (Ren et al., 2016; Xu et al., 2011). Irradiation experiments were also performed with pure water and DOM samples containing 10 mg/L NO_3^- . For most samples, NO_3^- photosensitization of $\cdot\text{OH}$ acted synergistically with DOM mediated photosensitization to increase the resulting pharmaceutical photodegradation rate. In the presence of an additional photosensitizer, DOM can compete for incident light, quench reactive intermediates and also reduce photooxidized intermediates (Miller and Chin, 2002; Wenk et al., 2011).

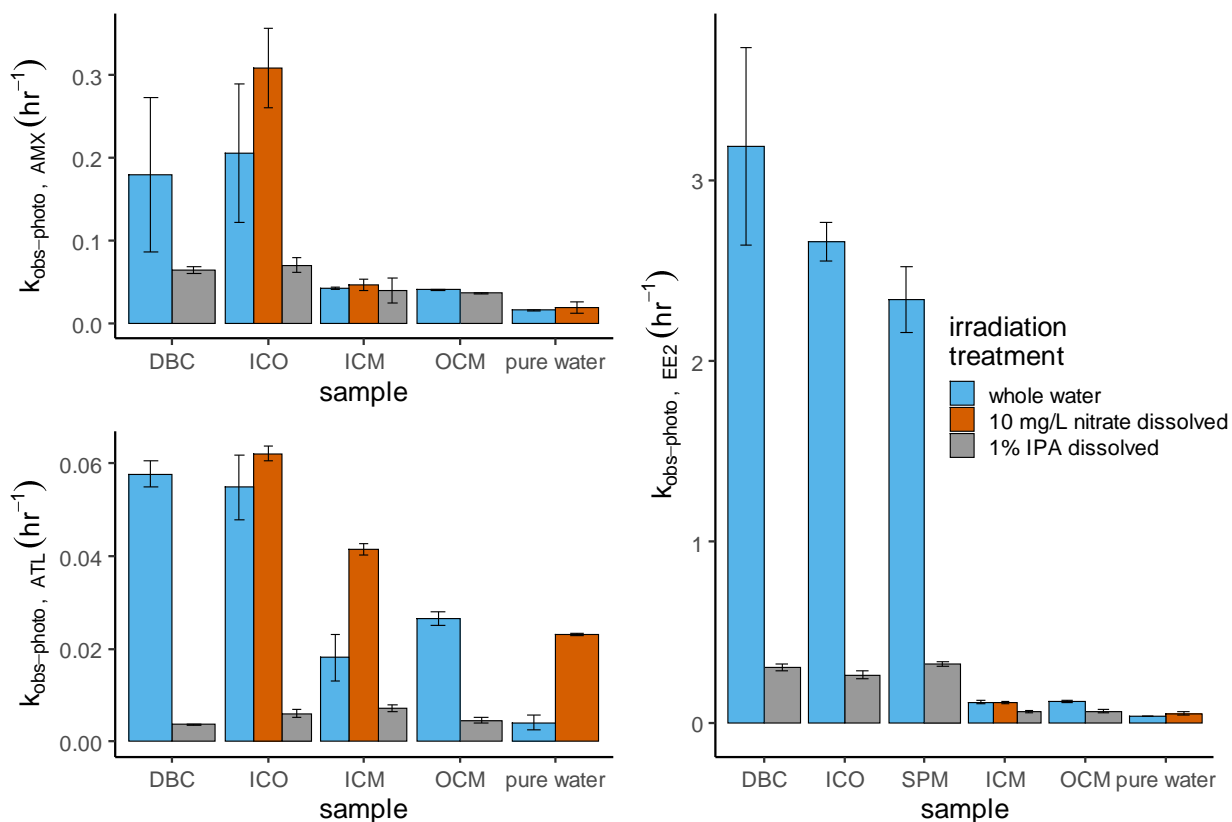


Figure 4: Phototransformation rates during irradiation experiments with hydroxyl radical ($\cdot\text{OH}$) quencher, 1% IPA (isopropyl alcohol) and hydroxyl radical photosensitizer, NO_3^- .

3.3 Optical properties and photoreactivity relationships

Optical properties derived from UV-Vis and EEM measurements are a part of photochemical studies and are used to quantify DOM characteristics and to develop predictive relationships with photoreactivity variables (Mckay et al., 2017; Timko et al., 2014). In this study, the rate of light absorption, R_a , was calculated to normalize the observed phototransformation rates between samples with diverse DOC and absorptivity. The normalization gives pharmaceutical specific quantum yield coefficients, $f_{\text{pharmaceutical}}$, which can be also used in correlation analysis between optical indices and photodegradation rates (Bodhipaksha et al., 2017). Higher $f_{\text{pharmaceutical}}$ indicates a higher efficiency of contaminant photodegradation per mole of light photons absorbed. In Figure 5, the range of photodegradation yields was highest for EE2, followed by CME, AMX, and then ATL. This implies that in sunlit wetland waters and wastewater effluents, the tendency to photodegrade is highest for EE2. The photoreactivity yields were grouped by sampling location and it was observed that lagoon treated wastewater had higher average values as compared to vegetated wetland cells and secondary effluents from NRRRF. A higher concentration of wastewater-like DOM in lagoon effluents leads to an overall increase in photoreactivity (Ryan et al., 2011; Wenk et al., 2019). Wastewater DOM has light absorbing chromophores which are more efficient than plant-derived and allochthonous terrestrial DOM in promoting photosensitization reactions (Lee et al., 2014; McCabe and Arnold, 2017; O'Connor et al., 2019).

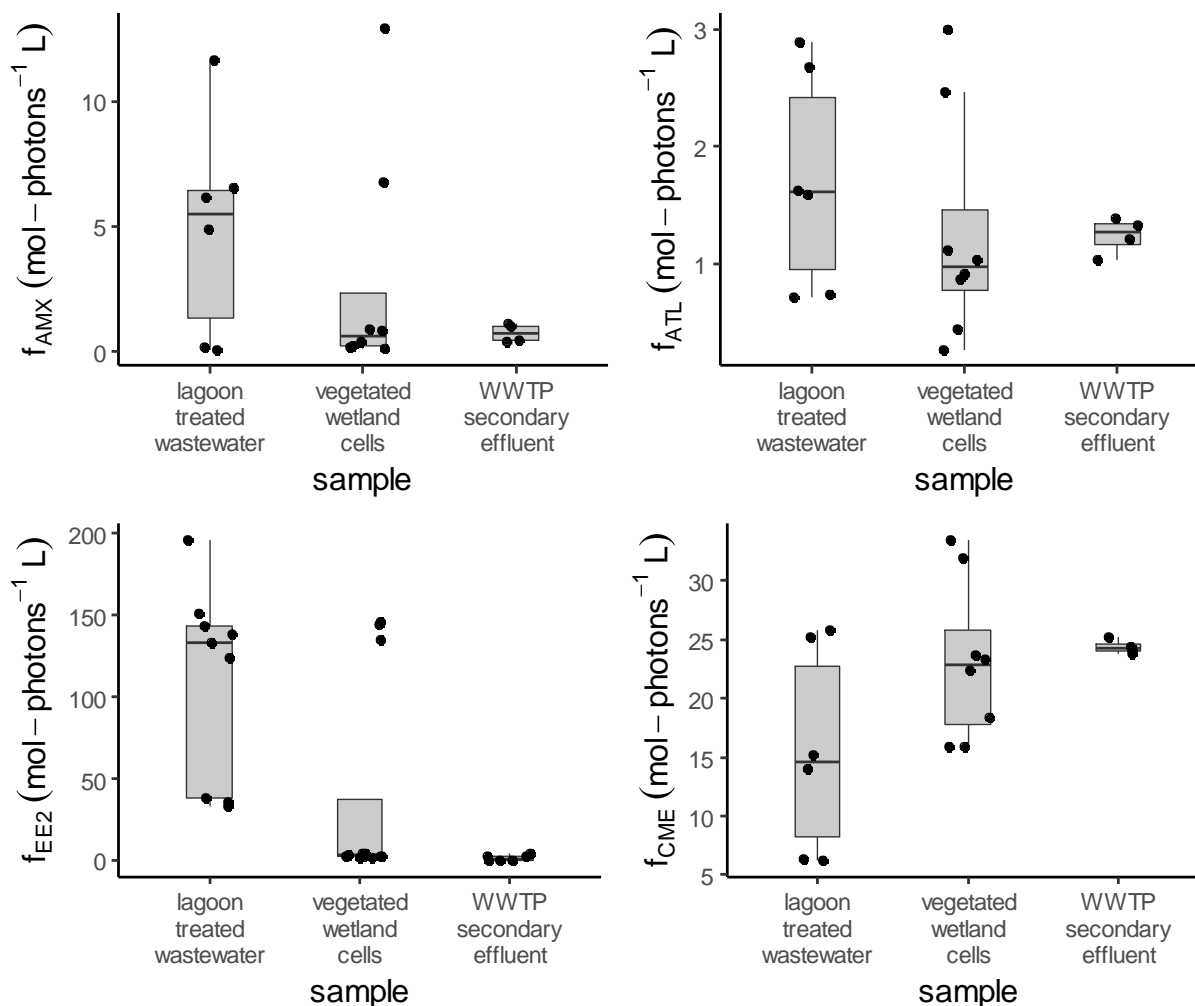


Figure 5: Quantum yield coefficient for the test compounds, $f_{\text{pharmaceutical}}$.

A matrix of Spearman's rank correlations between photoreactivity indicators and water chemistry and optical descriptors was prepared in the software R using the Hmisc package. A plot of this matrix is depicted in Figure 6 with statistically significant ($p < 0.05$) correlations displayed as colored circles. Blue circles represent positive correlations and negative correlations are shown in red. The color intensity and size of the circle is proportional to the correlation coefficients. The legend color indicates the strength of correlation (ρ) between two variables and the variables are ordered according to the correlation coefficient using a hierarchical clustering algorithm. The correlation analysis showed that peak fluorescence intensity of EEM regions and optical indicators of DOM source and processing had statistically significant correlations with pharmaceutical photoreactivity. Peaks A (UV humic-like), M (marine humic-like), and C (visible humic-like / fulvic-like) were negatively correlated to the photodegradation rates of atenolol (ATL) and 17 α -ethinyl-estradiol (EE2). Previous studies have shown that when $\cdot\text{OH}$ is the primary reactant, the presence of humic and fulvic DOM components can inhibit overall photodegradation rates of ATL and EE2. The decrease in photoreactivity could be due to quenching of photogenerated $\cdot\text{OH}$, screening of light, and reduction of contaminant intermediates (Chen et al., 2012; Ji et al., 2012;

Ren et al., 2017; Zeng et al., 2012). Cimetidine (CME) photodegradation was found to be positively correlated with E2:E3 and HIX, and negatively correlated with BIX and EEM peak T (tryptophan-like, protein-like). E2:E3 is the ratio of light absorbance at 250 nm to the absorbance at 365 nm and is negatively correlated to DOM molecular weight (Helms et al., 2008; Maizel et al., 2017). E2:E3 is regularly reported in studies as a suitable predictor of $^3\text{DOM}^*$ and $^1\text{O}_2$ photoreactivity and contaminant decay (Bodhipaksha et al., 2015; Mckay et al., 2017; O'Connor et al., 2019). Since CME photodegradation is entirely due to reactions with photogenerated $^1\text{O}_2$ an increase in E2:E3 correlated positively with phototransformation rates (Latch et al., 2003). For the subset of samples analyzed in irradiation experiments, the correlations of f_{CME} with HIX, BIX and EEM peak T were opposite to previous literature (McCabe and Arnold, 2018). The deviation can be because of effects specific to treatment wetlands and could be also due to biased $^1\text{O}_2$ quenching of stable sensitizers by DOM components (Mckay et al., 2016; Sharpless et al., 2014b).

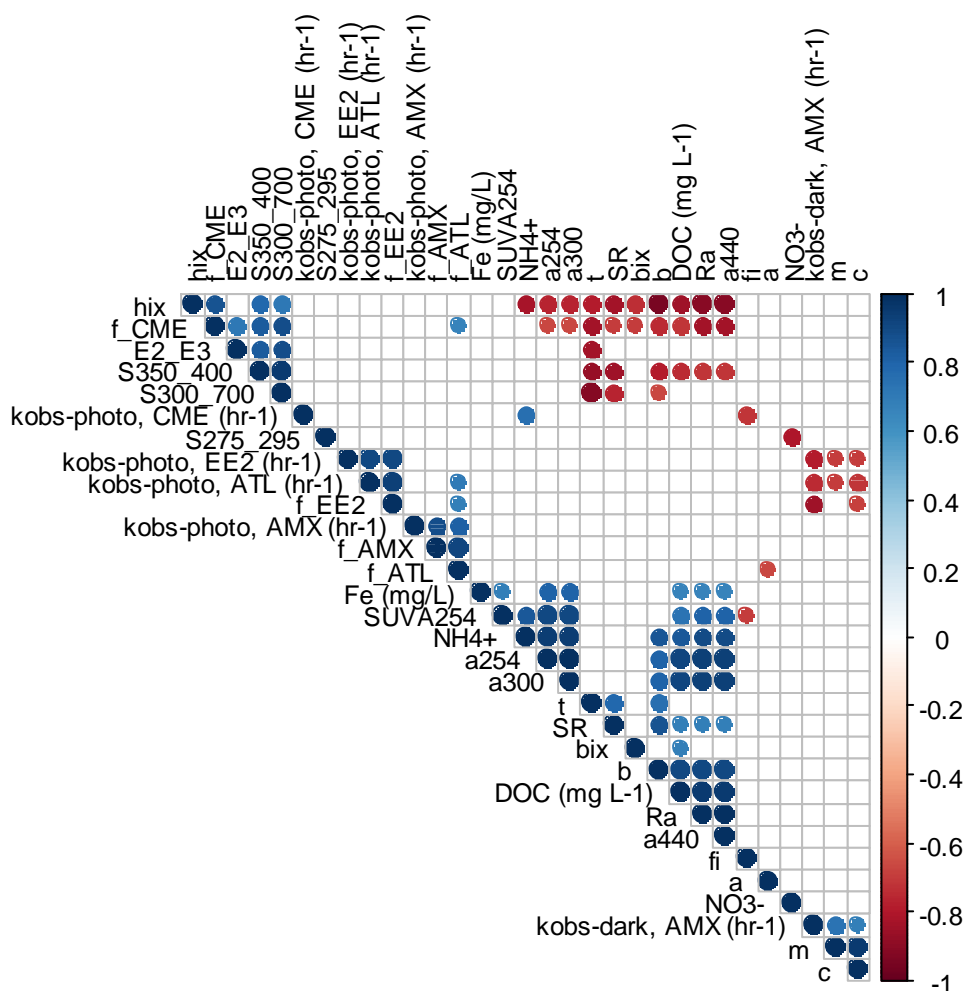


Figure 6: Spearman rank correlations coefficients (ρ) for statistically significant ($p < 0.05$) correlations between photodegradation rates, water quality, and DOM composition descriptors.

3.4 Coupling photochemical processes and wetland design

Photodegradation rate constants for pharmaceuticals observed during irradiation experiments were correlated to optical properties of waters sampled from treatment wetland cells and wastewater effluents. The main photoreactivity trend observed in this study was that photosensitized degradation of pharmaceuticals was higher in lagoon treated wastewater effluents than compared to samples from vegetated wetland cells and secondary wastewater effluents. It is suggested that from a unit process perspective, open-water cells should be placed before vegetated wetland cells to maximize photodegradation of contaminants (Wenk et al., 2019). Hydroxyl radical was the major reactant for amoxicillin, atenolol, and 17 α -ethynyl-estradiol (EE2), and was understood to be formed from both DOM mediated pathways and photo-Fenton mechanisms. The relatively higher presence of iron species at the Walnut Cove site could be a factor by which \cdot OH formation got enhanced from photo-Fenton reactions between photogenerated H₂O₂ and Fe(II) (Southworth and Voelker, 2003). Nitrate concentration was low in most samples analyzed, implying that the rate constants and quantum yield coefficients quantified in this study represent DOM as the only photosensitizer. The heterogeneous DOM sources and processing of DOM components at the Walnut Cove site can be hypothesized to be a reason for large variation in spectral properties and photosensitization yields (Sardana et al., 2019). The absorption spectra and photoreactivity yields of a representative wetland water were used to model phototransformation rates as a function of depth for a hypothetical open-water cell (Figure 7). Solar irradiance spectra at 40°N latitude for an average day in June and December was collected from Apell and McNeill, (2019). The modelled phototransformation rates of the pharmaceuticals were converted to half-life ($\ln(2)/k_{photo}$) estimates for an average day in June. Based on these simplified estimates for a 30 cm deep open-water wetland cell, the half-life was calculated to be 0.3 days for cimetidine, 1.8 days for 17 α -ethynyl-estradiol, 6.1 days for atenolol, and 7.5 days for amoxicillin. The kinetics of contaminant photodegradation were also applied to assess land area requirements for open-water wetland cells. The area needed to remove 90% of a contaminant via photodegradation was approximated using a modelling approach prescribed by Jasper and Sedlak, (2013). An average depth of 30 cm and a system flow rate of 0.2 MGD was assumed. The area required for 90% contaminant photodegradation in June was calculated to be 6.3 hectares for amoxicillin, 5.1 hectares for atenolol, 0.2 hectares for cimetidine, and 1.5 hectares for 17 α -ethynyl-estradiol. The Walnut Cove treatment site has multiple wetland cells with a total area of approximately 5 hectares. Thus, depending on photoreactivity and solar radiation, substantial removal of contaminants is possible via photodegradation in treatment wetland sites.

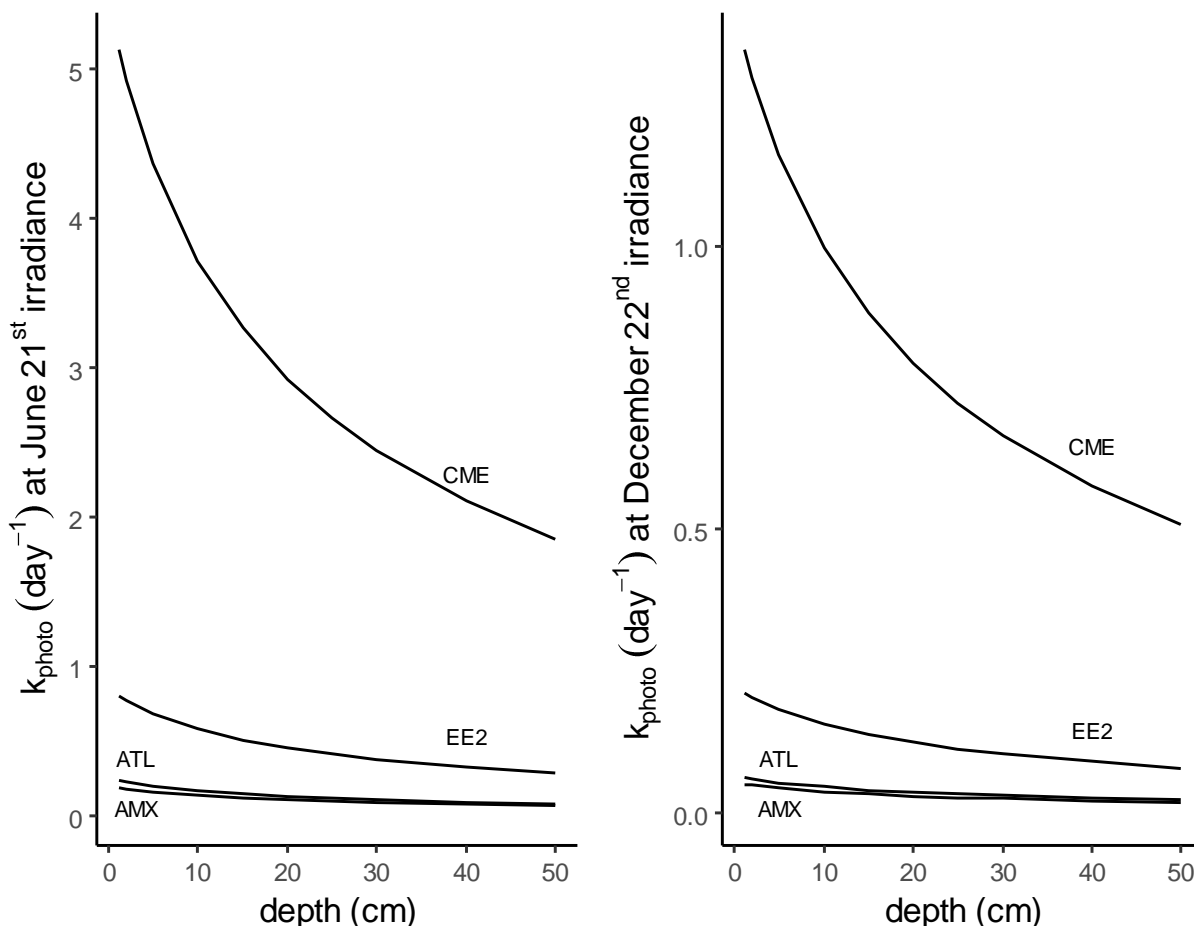


Figure 7: Estimated photodegradation rates in a treatment wetland for the selected pharmaceuticals as a function of depth.

4. Conclusions

This study evaluated the photodegradation of pharmaceuticals in treatment wetlands by using DOM characterization techniques and irradiation experiments. Phototransformation rates of atenolol (ATL), amoxicillin (AMX), and 17 α -ethynyl-estradiol (EE2) were determined to be higher in lagoon treated wastewaters than compared to vegetated wetland cells and secondary wastewater effluents. The main photoreactant responsible for the degradation of these pharmaceuticals in sampled waters was noted to be $\cdot\text{OH}$. Cimetidine (CME), which photodegrades mainly through $^1\text{O}_2$ had a uniform decay rate for all studied DOM compositions. DOM acted as the main photosensitizer since nitrate concentrations were negligible for most samples. Photoreactivity of some sampled waters was significantly higher due to enhanced $\cdot\text{OH}$ formation yields from photo-Fenton reactions and DOM dependent hydroxylators (Bodhipaksha et al., 2017; Page et al., 2011b). Optical descriptors of humic and fulvic DOM components were found to be negatively correlated with ATL and EE2 photoreactivity. E2:E3, which is often reported as a

predictor of photosensitization (Mckay et al., 2017), was found to be positively correlated only to CME phototransformation rates. It is suggested that plant-derived organic matter from vegetated wetland cells may reduce the photoreactivity potential of wastewater effluents through light screening, reactive intermediate quenching, and antioxidation effects (Miller and Chin, 2002; Wenk et al., 2019). For future work in the photochemistry of treatment wetlands, we suggest investigating the role of DOM composition on mechanisms and photoreactivity yields of reactive intermediates.

References

- Andreozzi, R., Caprio, V., Ciniglia, C., De Champdoré, M., Lo Giudice, R., Marotta, R., Zuccato, E., 2004. Antibiotics in the environment: Occurrence in Italian STPs, fate, and preliminary assessment on algal toxicity of amoxicillin. *Environ. Sci. Technol.* 38, 6832–6838. doi:10.1021/es049509a
- Andreozzi, R., Raffaele, M., Nicklas, P., 2003. Pharmaceuticals in STP effluents and their solar photodegradation in aquatic environment. *Chemosphere* 50, 1319–1330. doi:10.1016/S0045-6535(02)00769-5
- Apell, J.N., McNeill, K., 2019. Updated and validated solar irradiance reference spectra for estimating environmental photodegradation rates. *Environ. Sci. Process. Impacts* 21, 427–437. doi:10.1039/C8EM00478A
- Barber, L.B., Leenheer, J.A., Noyes, T.I., Stiles, E.A., 2001. Nature and Transformation of Dissolved Organic Matter in Treatment Wetlands. *Environ. Sci. Technol.* 35, 4805–4816. doi:10.1021/es010518i
- Bodhipaksha, L.C., Sharpless, C.M., Chin, Y.-P., MacKay, A.A., 2017. Role of effluent organic matter in the photochemical degradation of compounds of wastewater origin. *Water Res.* 110, 170–179. doi:10.1016/j.watres.2016.12.016
- Bodhipaksha, L.C., Sharpless, C.M., Chin, Y.-P., Sander, M., Langston, W.K., MacKay, A.A., 2015. Triplet Photochemistry of Effluent and Natural Organic Matter in Whole Water and Isolates from Effluent-Receiving Rivers. *Environ. Sci. Technol.* 49, 3453–3463. doi:10.1021/es505081w
- Brodin, T., Fick, J., Jonsson, M., Klaminder, J., 2013. Dilute concentrations of a psychiatric drug alter behavior of fish from natural populations. *Science* 339, 814–5. doi:10.1126/science.1226850
- Cass, Q.B., Gomes, R.F., Calafatti, S.A., Pedrazolli, J., 2003. Determination of amoxycillin in human plasma by direct injection and coupled-column high-performance liquid chromatography, in: *Journal of Chromatography A*. doi:10.1016/S0021-9673(02)01660-6
- Challis, J.K., Hanson, M.L., Friesen, K.J., Wong, C.S., 2014. A critical assessment of the photodegradation of pharmaceuticals in aquatic environments: defining our current understanding and identifying knowledge gaps. *Environ. Sci. Process. Impacts* 16, 672. doi:10.1039/c3em00615h
- Chen, W., Westerhoff, P., Leenheer, J.A., Booksh, K., 2003. Fluorescence Excitation–Emission Matrix Regional Integration to Quantify Spectra for Dissolved Organic Matter. *Environ. Sci. Technol.* 37, 5701–5710. doi:10.1021/es034354c
- Chen, Y., Li, Hong, Wang, Z., Li, Huijie, Tao, T., Zuo, Y., 2012. Photodegradation of selected β -blockers in aqueous fulvic acid solutions: Kinetics, mechanism, and product analysis. *Water Res.* 46, 2965–2972. doi:10.1016/J.WATRES.2012.03.025
- Chu, C., Lundeen, R.A., Remucal, C.K., Sander, M., McNeill, K., 2015. Enhanced Indirect Photochemical Transformation of Histidine and Histamine through Association with

- Chromophoric Dissolved Organic Matter. *Environ. Sci. Technol.* 49, 5511–5519. doi:10.1021/acs.est.5b00466
- Coble, P.G., 1996. Characterization of marine and terrestrial DOM in seawater using excitation-emission matrix spectroscopy. *Mar. Chem.* 51, 325–346. doi:10.1016/0304-4203(95)00062-3
- Coelho, C., Guyot, G., ter Halle, A., Cavani, L., Ciavatta, C., Richard, C., 2011. Photoreactivity of humic substances: relationship between fluorescence and singlet oxygen production. *Environ. Chem. Lett.* 9, 447–451. doi:10.1007/s10311-010-0301-3
- FENT, K., WESTON, A., CAMINADA, D., 2006. Ecotoxicology of human pharmaceuticals. *Aquat. Toxicol.* 76, 122–159. doi:10.1016/j.aquatox.2005.09.009
- Focazio, M.J., Kolpin, D.W., Barnes, K.K., Furlong, E.T., Meyer, M.T., Zaugg, S.D., Barber, L.B., Thurman, M.E., 2008. A national reconnaissance for pharmaceuticals and other organic wastewater contaminants in the United States — II) Untreated drinking water sources. *Sci. Total Environ.* 402, 201–216. doi:10.1016/J.SCITOTENV.2008.02.021
- Glassmeyer, S.T., Furlong, E.T., Kolpin, D.W., Batt, A.L., Benson, R., Boone, J.S., Conerly, O., Donohue, M.J., King, D.N., Kostich, M.S., Mash, H.E., Pfaller, S.L., Schenck, K.M., Simmons, J.E., Varughese, E.A., Vesper, S.J., Villegas, E.N., Wilson, V.S., 2017. Nationwide reconnaissance of contaminants of emerging concern in source and treated drinking waters of the United States. *Sci. Total Environ.* 581–582, 909–922. doi:10.1016/J.SCITOTENV.2016.12.004
- Helms, J.R., Stubbins, A., Perdue, E.M., Green, N.W., Chen, H., Mopper, K., 2013. Photochemical bleaching of oceanic dissolved organic matter and its effect on absorption spectral slope and fluorescence. *Mar. Chem.* 155, 81–91. doi:10.1016/j.marchem.2013.05.015
- Helms, J.R., Stubbins, A., Ritchie, J.D., Minor, E.C., Kieber, D.J., Mopper, K., 2008. Absorption spectral slopes and slope ratios as indicators of molecular weight, source, and photobleaching of chromophoric dissolved organic matter. *Limnol. Oceanogr.* 53, 955–969. doi:10.4319/lo.2008.53.3.0955
- Huguet, A., Vacher, L., Relexans, S., Saubusse, S., Froidefond, J.M., Parlanti, E., 2009. Properties of fluorescent dissolved organic matter in the Gironde Estuary. *Org. Geochem.* 40, 706–719. doi:10.1016/J.ORGGEOCHEM.2009.03.002
- Jasper, J.T., Nguyen, M.T., Jones, Z.L., Ismail, N.S., Sedlak, D.L., Sharp, J.O., Luthy, R.G., Horne, A.J., Nelson, K.L., 2013. Unit Process Wetlands for Removal of Trace Organic Contaminants and Pathogens from Municipal Wastewater Effluents. *Environ. Eng. Sci.* 30, 421–436. doi:10.1089/ees.2012.0239
- Jasper, J.T., Sedlak, D.L., 2013. Phototransformation of Wastewater-Derived Trace Organic Contaminants in Open-Water Unit Process Treatment Wetlands. *Environ. Sci. Technol.* 47, 10781–10790. doi:10.1021/es304334w
- Ji, Y., Zeng, C., Ferronato, C., Chovelon, J.-M., Yang, X., 2012. Nitrate-induced photodegradation of atenolol in aqueous solution: Kinetics, toxicity and degradation pathways. *Chemosphere* 88, 644–649. doi:10.1016/J.CHEMOSPHERE.2012.03.050

- Karpuzcu, M.E., McCabe, A.J., Arnold, W.A., 2016. Phototransformation of pesticides in prairie potholes: effect of dissolved organic matter in triplet-induced oxidation. *Environ. Sci. Process. Impacts* 18, 237–245. doi:10.1039/C5EM00374A
- Kidd, K.A., Blanchfield, P.J., Mills, K.H., Palace, V.P., Evans, R.E., Lazorchak, J.M., Flick, R.W., 2007. Collapse of a fish population after exposure to a synthetic estrogen. *Proc. Natl. Acad. Sci. U. S. A.* 104, 8897–901. doi:10.1073/pnas.0609568104
- Kolpin, D.W., Furlong, E.T., Meyer, M.T., Thurman, E.M., Zaugg, S.D., Barber, L.B., Buxton, H.T., 2002. Pharmaceuticals, hormones, and other organic wastewater contaminants in U.S. streams, 1999–2000: a national reconnaissance. *Environ. Sci. Technol.* 36, 1202–11. doi:10.1021/es011055j
- Küster, A., Alder, A.C., Escher, B., Duis, K., Fenner, K., Garric, J., Hutchinson, T., Lapen, D., Péry, A., Römbke, J., Snape, J., Ternes, T., Topp, E., Wehrhan, A., Knacker, T., 2007. Environmental Risk Assessment of Human Pharmaceuticals in the European Union - A Case Study with the β -blocker Atenolol. *Integr. Environ. Assess. Manag.* preprint, 1. doi:10.1897/IEAM_2009-050.1
- Laszakovits, J.R., Berg, S.M., Anderson, B.G., O'Brien, J.E., Wammer, K.H., Sharpless, C.M., 2017. p-Nitroanisole/Pyridine and p-Nitroacetophenone/Pyridine Actinometers Revisited: Quantum Yield in Comparison to Ferrioxalate. *Environ. Sci. Technol. Lett.* 4, 11–14. doi:10.1021/acs.estlett.6b00422
- Latch, D.E., Stender, B.L., Packer, J.L., Arnold, W.A., McNeill, K., 2003. Photochemical fate of pharmaceuticals in the environment: cimetidine and ranitidine. *Environ. Sci. Technol.* 37, 3342–50. doi:10.1021/es0340782
- Lee, E., Shon, H.K., Cho, J., 2014. Role of wetland organic matters as photosensitizer for degradation of micropollutants and metabolites. *J. Hazard. Mater.* 276, 1–9. doi:10.1016/j.jhazmat.2014.05.001
- Leifer, A., 1989. The Kinetics of Environmental Aquatic Photochemistry. *Anal. Chem.* 61, 220A–220A. doi:10.1021/ac00178a769
- Liu, Q.-T., Williams, H.E., 2007. Kinetics and Degradation Products for Direct Photolysis of β -Blockers in Water. *Environ. Sci. Technol.* 41, 803–810. doi:10.1021/es0616130
- Maie, N., Jaffé, R., Miyoshi, T., Childers, D.L., 2006. Quantitative and Qualitative Aspects of Dissolved Organic Carbon Leached from Senescent Plants in an Oligotrophic Wetland. *Biogeochemistry* 78, 285–314. doi:10.1007/s10533-005-4329-6
- Maizel, A.C., Li, J., Remucal, C.K., 2017. Relationships Between Dissolved Organic Matter Composition and Photochemistry in Lakes of Diverse Trophic Status. *Environ. Sci. Technol.* 51, 9624–9632. doi:10.1021/acs.est.7b01270
- Matamoros, V., García, J., Bayona, J.M., 2008. Organic micropollutant removal in a full-scale surface flow constructed wetland fed with secondary effluent. *Water Res.* 42, 653–660. doi:10.1016/J.WATRES.2007.08.016
- Matamoros, V., Salvadó, V., 2012. Evaluation of the seasonal performance of a water reclamation pond-constructed wetland system for removing emerging contaminants. *Chemosphere* 86,

111–7. doi:10.1016/j.chemosphere.2011.09.020

- McCabe, A.J., Arnold, W.A., 2018. Multiple linear regression models to predict the formation efficiency of triplet excited states of dissolved organic matter in temperate wetlands. *Limnol. Oceanogr.* 63, 1992–2014. doi:10.1002/lno.10820
- McCabe, A.J., Arnold, W.A., 2017. Reactivity of Triplet Excited States of Dissolved Natural Organic Matter in Stormflow from Mixed-Use Watersheds. *Environ. Sci. Technol.* 51, 9718–9728. doi:10.1021/acs.est.7b01914
- Mckay, G., Couch, K.D., Mezyk, S.P., Rosario-Ortiz, F.L., 2016. Investigation of the Coupled Effects of Molecular Weight and Charge-Transfer Interactions on the Optical and Photochemical Properties of Dissolved Organic Matter. *Environ. Sci. Technol.* 50, 8093–8102. doi:10.1021/acs.est.6b02109
- Mckay, G., Huang, W., Romera-Castillo, C., Crouch, J.E., Rosario-Ortiz, F.L., Jaffé, R., 2017. Predicting Reactive Intermediate Quantum Yields from Dissolved Organic Matter Photolysis Using Optical Properties and Antioxidant Capacity. *Environ. Sci. Technol.* 51, 5404–5413. doi:10.1021/acs.est.6b06372
- McKnight, D.M., Boyer, E.W., Westerhoff, P.K., Doran, P.T., Kulbe, T., Andersen, D.T., 2001. Spectrofluorometric characterization of dissolved organic matter for indication of precursor organic material and aromaticity. *Limnol. Oceanogr.* 46, 38–48. doi:10.4319/lo.2001.46.1.0038
- Miller, P.L., Chin, Y.-P., 2002. Photoinduced Degradation of Carbaryl in a Wetland Surface Water. *J. Agric. Food Chem.* 50, 6758–6765. doi:10.1021/jf025545m
- O'Connor, M., Helal, S.R., Latch, D.E., Arnold, W.A., 2019. Quantifying photo-production of triplet excited states and singlet oxygen from effluent organic matter. *Water Res.* 156, 23–33. doi:10.1016/j.watres.2019.03.002
- Ohno*, T., 2002. Fluorescence Inner-Filtering Correction for Determining the Humification Index of Dissolved Organic Matter. doi:10.1021/ES0155276
- Page, S.E., Arnold, W.A., McNeill, K., 2011a. Assessing the Contribution of Free Hydroxyl Radical in Organic Matter-Sensitized Photohydroxylation Reactions. *Environ. Sci. Technol.* 45, 2818–2825. doi:10.1021/es2000694
- Page, S.E., Arnold, W.A., McNeill, K., 2011b. Assessing the Contribution of Free Hydroxyl Radical in Organic Matter-Sensitized Photohydroxylation Reactions. *Environ. Sci. Technol.* 45, 2818–2825. doi:10.1021/es2000694
- Pereira, V.J., Linden, K.G., Weinberg, H.S., 2007. Evaluation of UV irradiation for photolytic and oxidative degradation of pharmaceutical compounds in water. *Water Res.* 41, 4413–4423. doi:10.1016/J.WATRES.2007.05.056
- Peterson, B.M., McNally, A.M., Cory, R.M., Thoemke, J.D., Cotner, J.B., McNeill, K., 2012. Spatial and temporal distribution of singlet oxygen in Lake Superior. *Environ. Sci. Technol.* 46, 7222–7229. doi:10.1021/es301105e
- Pinney, M.L., Westerhoff, P.K., Baker, L., 2000. Transformations in dissolved organic carbon

- through constructed wetlands. *Water Res.* 34, 1897–1911. doi:10.1016/S0043-1354(99)00330-9
- Pucher, M., Wünsch, U., Weigelhofer, G., Murphy, K., Hein, T., Graeber, D., 2019. staRdom: Versatile Software for Analyzing Spectroscopic Data of Dissolved Organic Matter in R. *Water* 11, 2366. doi:10.3390/w11112366
- Ren, D., Chen, F., Ren, Z., Wang, Y., 2019a. Different response of 17 α -ethynylestradiol photodegradation induced by aquatic humic and fulvic acids to typical water matrixes. *Process Saf. Environ. Prot.* 121, 367–373. doi:10.1016/J.PSEP.2018.11.018
- Ren, D., Huang, B., Bi, T., Xiong, D., Pan, X., 2016. Effects of pH and dissolved oxygen on the photodegradation of 17 α -ethynylestradiol in dissolved humic acid solution. *Environ. Sci. Process. Impacts* 18, 78–86. doi:10.1039/C5EM00502G
- Ren, D., Huang, B., Xiong, D., He, H., Meng, X., Pan, X., 2017. Photodegradation of 17 α -ethynylestradiol in dissolved humic substances solution: Kinetics, mechanism and estrogenicity variation. *J. Environ. Sci. (China)* 54, 196–205. doi:10.1016/j.jes.2016.03.002
- Ren, D., Ren, Z., Chen, F., Wang, B., Huang, B., 2019b. Predictive role of spectral slope ratio towards 17 α -ethynylestradiol photodegradation sensitized by humic acids. *Environ. Pollut.* 254, 112959. doi:10.1016/J.ENVPOL.2019.112959
- Rosario-Ortiz, F.L., Wert, E.C., Snyder, S.A., 2010. Evaluation of UV/H₂O₂ treatment for the oxidation of pharmaceuticals in wastewater. *Water Res.* 44, 1440–1448. doi:10.1016/J.WATRES.2009.10.031
- Ryan, C.C., Tan, D.T., Arnold, W.A., 2011. Direct and indirect photolysis of sulfamethoxazole and trimethoprim in wastewater treatment plant effluent. *Water Res.* 45, 1280–1286. doi:10.1016/j.watres.2010.10.005
- Sardana, A., Cottrell, B., Soulsby, D., Aziz, T.N., 2019. Dissolved organic matter processing and photoreactivity in a wastewater treatment constructed wetland. *Sci. Total Environ.* 648, 923–934. doi:10.1016/j.scitotenv.2018.08.138
- Schwarzenbach, R.P., Escher, B.I., Fenner, K., Hofstetter, T.B., Johnson, C.A., von Gunten, U., Wehrli, B., 2006. The challenge of micropollutants in aquatic systems. *Science* 313, 1072–7. doi:10.1126/science.1127291
- Schwarzenbach, R.P., Gschwend, P.M., Imboden, D.M., 2002. *Environmental Organic Chemistry*, Environmental Organic Chemistry. John Wiley & Sons, Inc., Hoboken, NJ, USA, NJ, USA. doi:10.1002/0471649643
- Sharpless, C.M., Aeschbacher, M., Page, S.E., Wenk, J., Sander, M., McNeill, K., 2014a. Photooxidation-Induced Changes in Optical, Electrochemical, and Photochemical Properties of Humic Substances. *Environ. Sci. Technol.* 48, 2688–2696. doi:10.1021/es403925g
- Sharpless, C.M., Aeschbacher, M., Page, S.E., Wenk, J., Sander, M., McNeill, K., 2014b. Photooxidation-Induced Changes in Optical, Electrochemical, and Photochemical Properties of Humic Substances. *Environ. Sci. Technol.* 48, 2688–2696. doi:10.1021/es403925g
- Silverman, A.I., Nguyen, M.T., Schilling, I.E., Wenk, J., Nelson, K.L., 2015. Sunlight inactivation

- of viruses in open-water unit process treatment wetlands: modeling endogenous and exogenous inactivation rates. *Environ. Sci. Technol.* 49, 2757–66. doi:10.1021/es5049754
- Snyder, S.A., Westerhoff, P., Yoon, Y., Sedlak, D.L., 2003. Pharmaceuticals, Personal Care Products, and Endocrine Disruptors in Water: Implications for the Water Industry. *Environ. Eng. Sci.* 20, 449–469. doi:10.1089/109287503768335931
- Song, W., Chen, W., Cooper, W.J., Greaves, J., Miller, G.E., 2008. Free-Radical Destruction of β -Lactam Antibiotics in Aqueous Solution. *J. Phys. Chem. A* 112, 7411–7417. doi:10.1021/jp803229a
- Southworth, B.A., Voelker, B.M., 2003. Hydroxyl radical production via the photo-fenton reaction in the presence of fulvic acid. *Environ. Sci. Technol.* 37, 1130–1136. doi:10.1021/es0207571
- Timko, S.A., Romera-Castillo, C., Jaffé, R., Cooper, W.J., 2014. Photo-reactivity of natural dissolved organic matter from fresh to marine waters in the Florida Everglades, USA. *Environ. Sci. Process. Impacts* 16, 866–78. doi:10.1039/c3em00591g
- Vajda, A.M., Barber, L.B., Gray, J.L., Lopez, E.M., Woodling, J.D., Norris, D.O., 2008. Reproductive Disruption in Fish Downstream from an Estrogenic Wastewater Effluent. *Environ. Sci. Technol.* 42, 3407–3414. doi:10.1021/es0720661
- Verlicchi, P., Zambello, E., 2014. How efficient are constructed wetlands in removing pharmaceuticals from untreated and treated urban wastewaters? A review. *Sci. Total Environ.* 470–471, 1281–1306. doi:10.1016/j.scitotenv.2013.10.085
- Vermilyea, A.W., Voelker, B.M., 2009. Photo-Fenton Reaction at Near Neutral pH. *Environ. Sci. Technol.* 43, 6927–6933. doi:10.1021/es900721x
- Vymazal, J., 2007. Removal of nutrients in various types of constructed wetlands. *Sci. Total Environ.* 380, 48–65. doi:10.1016/j.scitotenv.2006.09.014
- Wang, L., Xu, H., Cooper, W.J., Song, W., 2012. Photochemical fate of beta-blockers in NOM enriched waters. *Sci. Total Environ.* 426, 289–95. doi:10.1016/j.scitotenv.2012.03.031
- Weishaar, J.L., Aiken, G.R., Bergamaschi, B.A., Fram, M.S., Fujii, R., Mopper, K., 2003. Evaluation of Specific Ultraviolet Absorbance as an Indicator of the Chemical Composition and Reactivity of Dissolved Organic Carbon. *Environ. Sci. Technol.* 37, 4702–4708. doi:10.1021/es030360x
- Wenk, J., Nguyen, M.T., Nelson, K.L., 2019. Natural Photosensitizers in Constructed Unit Process Wetlands: Photochemical Characterization and Inactivation of Pathogen Indicator Organisms. *Environ. Sci. Technol.* 53, 7724–7735. doi:10.1021/acs.est.9b01180
- Wenk, J., von Gunten, U., Canonica, S., 2011. Effect of Dissolved Organic Matter on the Transformation of Contaminants Induced by Excited Triplet States and the Hydroxyl Radical. *Environ. Sci. Technol.* 45, 1334–1340. doi:10.1021/es102212t
- Xu, H., Cooper, W.J., Jung, J., Song, W., 2011. Photosensitized degradation of amoxicillin in natural organic matter isolate solutions. *Water Res.* 45, 632–8. doi:10.1016/j.watres.2010.08.024

- Yamamoto, H., Nakamura, Yudai, Moriguchi, S., Nakamura, Yuki, Honda, Y., Tamura, I., Hirata, Y., Hayashi, A., Sekizawa, J., 2009. Persistence and partitioning of eight selected pharmaceuticals in the aquatic environment: Laboratory photolysis, biodegradation, and sorption experiments. *Water Res.* doi:10.1016/j.watres.2008.10.039
- Yoon, K.H., Lee, S.Y., Kim, W., Park, J.S., Kim, H.J., 2004. Simultaneous determination of amoxicillin and clavulanic acid in human plasma by HPLC-ESI mass spectrometry. *J. Chromatogr. B Anal. Technol. Biomed. Life Sci.* doi:10.1016/j.jchromb.2004.09.018
- Zeng, C., Ji, Y., Zhou, L., Zhang, Y., Yang, X., 2012. The role of dissolved organic matters in the aquatic photodegradation of atenolol. *J. Hazard. Mater.* 239–240, 340–347. doi:10.1016/j.jhazmat.2012.09.005
- Zenobio, J.E., Sanchez, B.C., Leet, J.K., Archuleta, L.C., Sepúlveda, M.S., 2015. Presence and effects of pharmaceutical and personal care products on the Baca National Wildlife Refuge, Colorado. *Chemosphere.* doi:10.1016/j.chemosphere.2014.10.050
- Zhang, L., Lyu, T., Zhang, Y., Button, M., Arias, C.A., Weber, K.P., Brix, H., Carvalho, P.N., 2018. Impacts of design configuration and plants on the functionality of the microbial community of mesocosm-scale constructed wetlands treating ibuprofen. *Water Res.* 131, 228–238. doi:10.1016/j.watres.2017.12.050